



# Azo Dye Removal from Aqueous Solutions Using Laccase-modified Red Mud: Adsorption Kinetics and Isotherm Studies

H. Nadaroglu<sup>1\*</sup>, E. Kalkan<sup>2</sup> and N. Celebi<sup>1</sup>

<sup>1</sup>Ataturk University, Erzurum Vocational Training School, 25240 Erzurum, Turkey.

<sup>2</sup>Ataturk University, Oltu Earth Sciences Faculty, Geological Engineering Department, 25400 Oltu-Erzurum, Turkey.

## Authors' contributions

*This work was carried out in collaboration between all authors. Author HN designed the study, performed the statistical analysis, wrote the protocol and wrote the first draft of the manuscript. Author NC managed the analyses of the study. Author EK managed the literature searches. All authors read and approved the final manuscript.*

Original Research Article

Received 14<sup>th</sup> March 2014  
Accepted 7<sup>th</sup> April 2014  
Published 6<sup>th</sup> May 2014

## ABSTRACT

Removal of acid red 37 from aqueous solutions has been studied using red mud waste material after its modification with laccase from Russulaceae (*Lactarius volemus*). Laccase was purified by using saturated precipitate (NH<sub>4</sub>)<sub>2</sub>SO<sub>4</sub>, diethylaminoethyl cellulose (DEAE-cellulose) and immobilized on red mud. The removal of acid red 37 by the laccase-modified red mud has been demonstrated in order to explore its potential use as low-cost adsorbent. The adsorption kinetics of acid red 37 dye on the laccase-modified red mud with respect to pH, contact time, temperature and adsorbent dose were investigated. The optimum results were obtained at pH 4, contact time of 60 min and temperature of 30°C. The Freundlich equation was found to have the highest value of R<sup>2</sup> compared with the Langmuir model. Thermodynamic parameters including the Gibbs free energy, enthalpy and entropy changes indicated that the adsorption of acid red 37 onto laccase-modified red mud was feasible, spontaneous and endothermic.

**Keywords:** *Laccase-modified red mud; acid red 37; dye removal; adsorption isotherm; wastewater.*

\*Corresponding author: Email: [hnisa25@atauni.edu.tr](mailto:hnisa25@atauni.edu.tr);

## **1. INTRODUCTION**

The textile industry consumes considerable amounts of water during dyeing and finishing operations. Its effluents are usually strongly colored, containing high concentrations of dyes, tensoactive compounds, chromium, suspended solids and high chemical oxygen demand. The presence of dyestuff in textile wastewater is aesthetically offensive, inhibits photosynthetic processes in water bodies and, in many cases, generates toxicity to aquatic organisms and humans. Most dyes contained in textile effluents are designed to resist oxidizing and reducing agents, washing and light exposure. These characteristics make such chemicals highly refractory and hard to remove by using conventional wastewater treatment processes [1-4].

Textile-processing industries largely employ azo dyes. They are aromatic hydrocarbons, derivatives of benzene, toluene, naphthalene, phenol and aniline [5]. Azo dye has an azo group bond (-N=N-) and because of their low cost, variety, solubility and stability are the most common synthetic dye that have been used for dyeing [5]. It is estimated that over 50% of total produced dye in world is azo dye. It has been recognized that between 1–20% of the whole world production of azo dyes is lost during the dyeing processes and providing main wastewater pollution in wastewaters. There are aromatic rings in the azo dye molecular structures which cause these effluents to be toxic and mostly non-biodegradable; therefore, becoming an important source of environmental pollution [6-8]. Approximately 10-15% of the overall production of azo dyes is released into the environment, mainly via wastewater [9]. This is very dangerous because some of the azo dyes and their degradation products have a toxic, mutagenic or carcinogenic influence on living organisms. Therefore, the azo dye-containing wastewater should be treated before discharge [10-13].

Recently, physicochemical methods have been used for removal of dyes in wastewaters though, these methods are economically unviable, environmentally unfriendly and results in generation of residual sludge [14,15]. Consequently, amongst numerous techniques, adsorption techniques seem to have the most potential for future use in industrial wastewater treatment because of their proven efficiency in the removal of organic and mineral pollutants and for economic considerations [16,17]. Activated carbon is the most widely used adsorbent for this purpose because it has a high capacity for adsorption of color but its use is limited because of high cost. The removal of dyes from effluent using adsorption process provide an alternative treatment, especially if the adsorbent is inexpensive and readily available [18-21]. An adsorbent can be considered as cheap or low-cost if it is abundant in nature, requires little processing and is a byproduct of waste material from industrial waste [22]. Many low-cost adsorbents have been investigated on dye removal, such as orange peel [23], bottom ash [24-27], red mud [27], silica fume [28,29], clay [30], zeolite [26,31], calcine alunite [32], peanut hull [31], rice husk [33].

As an alternative low-cost adsorbent material, solid wastes are generally used as adsorbent for the remediation of wastewater. One type of solid waste materials, red mud (RM), is largely produced from the alumina industry. The RM emerges as a by-product of the caustic leaching of bauxite to produce alumina. This material is principally composed of fine particles of silica, aluminum, iron, calcium and titanium oxides and hydroxides, which are responsible for its high surface reactivity [34,35]. Because of these characteristics, RM has been the subject of many investigations, including some on the removal of toxic heavy metals from wastewater and acid mine drainage or on reducing the leaching of soil nutrients [18,19,36, 37]. It has been noted in the literature that the RM could be used for decontaminating mining

sites and other contaminated areas, which generate acidic leachates and produce high concentrations of hazardous heavy metal ions [38].

Laccase is an enzyme that has potential ability of oxidation. It belongs to those enzymes, which have innate properties of reactive radical production [39]. There are diverse sources of laccase producing organisms like bacteria, fungi and plants. Laccases use oxygen and produce water as by product. They can degrade a range of compounds including phenolic and non-phenolic compounds. They also have ability to detoxify a range of environmental pollutants [39]. Laccases are produced by the majority of white-rot fungi described to-date as well as by other types of fungi and plants, insects and some bacteria. Fungal laccases are believed to be involved in the degradation of lignin, the removal of potentially toxic phenols arising during lignin degradation, the fruit body development, pigment production and antimicrobial activity [40,41].

In the present study describes the use of laccase modified-RM for removal of acid red 37 (AR37) dye from aqueous solutions. The adsorption of AR37 dye has been investigated as a function of contact time, pH, temperature and adsorbent dose. The AR37 azo dye has been absorbed by laccase modified-RM from AR37 dye polluted-wastewater. Adsorption isotherm, kinetic and thermodynamic studies have been performed to describe the adsorption process.

## 2. MATERIALS AND METHODS

### 2.1 AR37 Textile Dye

The wastewater including AR37 textile dye was purchased from Erzurum Industrial Area (Turkey) and used the experimental study. AR37 dye is dissociated anionic sulfonate in aqueous solution with the molecular structure. It is used mainly in dyes for wool manufacturing, wood coatings, silk and leather [42,43]. The chemical structure and the general characteristics of AR37 are summarized in Fig. 1 and Table 1, respectively.

**Table 1. General characteristics of AR37 dye**

Chemical formula	Molar mass	Color index number	$\lambda_{\max}$
$C_{18}H_{14}N_4Na_2O_8S_2$	524.44 g/mol	17045	504 nm

### 2.2 Purification of Laccase Enzyme

20 g *Lactarius volemus* was ground in liquid  $N_2$  and then homogenized in a blender with 50 mL of 1 M KCl by shaking, and centrifuged at 5.000xg for 60 min. The homogenates were centrifuged and precipitates were removed. For the purification of the laccase enzyme the following procedure was implemented [44]. Laccase was purified from the supernatant in two steps. Firstly, it was partially purified by precipitation % in  $(NH_4)_2SO_4$ . Secondly, ion exchange chromatography on DEAE-sephadex was used. The collapse of  $(NH_4)_2SO_4$  was done from 0% to 90% in supernatant with the internal of 0-10, 10-20, 20-30, 30-40, 40-50, 50-60, 60-70, 70-80 and 80-90. Significant activity was not observed below at a range 0-40%  $(NH_4)_2SO_4$ . The majority of activity was found in the 40-60% precipitate. Solid  $(NH_4)_2SO_4$  was added to the supernatant to increase the concentration of  $(NH_4)_2SO_4$  from 40% the fraction to 60%. After, mixing it in an ice-bath for 1 h with magnetic stirring, it was centrifuged (10.000 x g, 30 min and 4°C). The supernatant was discarded and the precipitate was dissolved in 0.01 M acetate buffer (pH 5.0) and dialyzed against the same buffer [44,45].

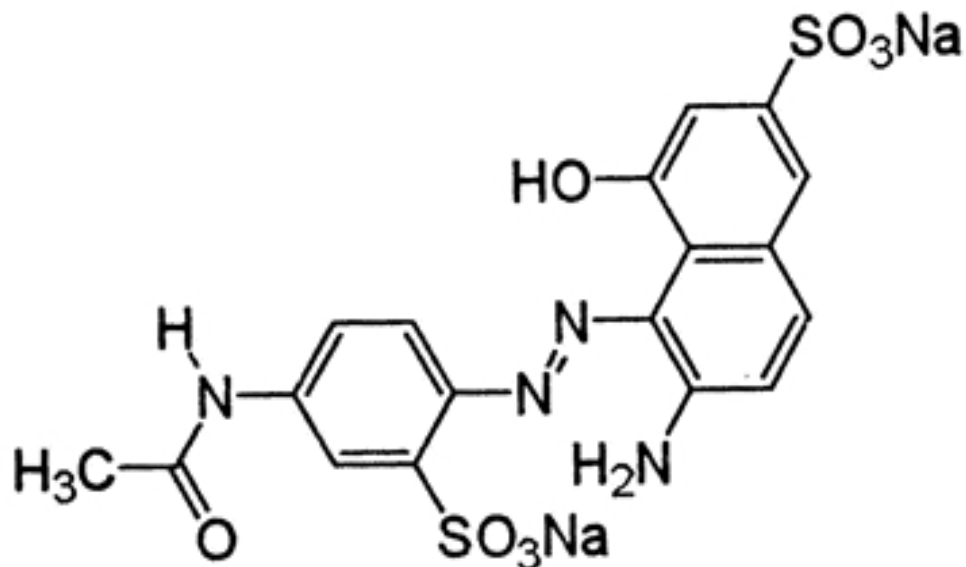


**Fig. 1. Chemical structure of AR37 (trisodium (4Z)-3-oxo-4-[(4-sulfonatophthalen-1-yl)hydrazinylidene]naphthalene-2,7-disulfonate) dye**

### 2.3 Anion Exchange Chromatography

The dialyzed suspension after ammonium sulfate precipitation from the above step was subjected to anion exchange chromatography on DEAE-sephadex fast flow column (2,5 x 30 cm) pre-equilibrated with 0.02 M acetate buffer pH 5.0. The column was washed thoroughly with the same buffer until no protein was detected in the eluate. The bound proteins were eluted with the same buffer using a linear gradient of NaCl from 0 M to 2 M. Fractions of 3 mL volume were collected at a flow rate of 3 mL/min. Protein elution was monitored spectrophotometrically by measuring the absorbance at 280 nm. Activity was measured by using 2,2'-Azino-bis(3-ethylbenzothiazoline-6-sulfonic acid) (ABTS) as the assay substrate. The active fractions from each peak were pooled and stored at 4 °C. Protein concentration was determined spectrophotometrically (absorbance at 280 nm) as well as by Bradford's method [46], using bovine serum albumin (BSA) as the standard.

The reagent 2,2'-azino-di-[3-ethyl-benzothiazolin-sulfonate] (ABTS) was used as a substrate for spectrophotometric determination of laccase activity [47,48]. One activity unit (U) was the amount of enzyme that oxidized 1  $\mu$ mol of ABTS  $\text{min}^{-1}$  and the activities were expressed in  $\text{U l}^{-1}$ .

### 2.4 Sodium Dodecyl Sulphate Polyacrylamide (SDS-PAGE) gel Electrophoresis

The SDS polyacrylamide gel electrophoresis was performed after the purification of the enzyme. It was carried out in 3% and 10% acrylamide concentrations for the stacking and running gels, respectively, each of them containing 0.1% SDS [49]. The sample (20  $\mu$ g) was applied to the electrophoresis medium. Bromo tymol blue was used as tracking dye. Gels were stained in 0.1% Coomassie Brilliant Blue R-250 in 50% methanol, 10% acetic acid and

40% distilled water for 1.5 h. It was destained by washing with 50% methanol, 10% acetic acid and 40% distilled water several times. The electrophoretic pattern was photographed (Fig. 2).



**Fig. 2. SDS-PAGE electrophoretic pattern of laccase [homogenate (I); standart protein (bovine serum albumin, 66 kDa; egg ovalbumin, 45 kDa; pepsin, 34 kDa; trypsinogen, 29 kDa; carbonic anhydrase) (II); purified laccase enzyme from Russulaceae (*Lactarius volemus*) (III)]**

## 2.5 Molecular Weight Determination by Gel Filtration

A column (3x70 cm) of Sephadex G100 was prepared. The column was equilibrated with the buffer (0.05 M Na<sub>2</sub>HPO<sub>4</sub>, 1 mM dithioerythretol, pH 7) until the absorbance was zero at 280 nm. The standard protein solution (bovine serum albumin, 66 kDa; egg ovalbumin, 45 kDa; pepsin, 34 kDa; trypsinogen, 24 kDa; β-lactoglobulin and lysozyme, 14 kDa) was added to the column. The purified laccase enzyme was added into the column separately and then eluted under the same conditions. The flow rate through the column was 20 mL/h. The elution volume was compared with standard proteins [50].

## 2.6 Adsorbent and its Preparation for Experimental Study

The alkaline RM-water pump is dumped annually into specially constructed dams around the Seydisehir Aluminum Plant (Konya, Turkey). The RM used in this experimental study has been obtained from this plant. Its physical properties, chemical composition and mineralogical composition are given in Table 2.

**Table 2. Physical property, chemical constituent and mineralogical composition of RM**

	<b>Value</b>
<b>Properties</b>	
Density (mg/m <sup>3</sup> )	28.50
Specific gravity	3.05
pH	12-13
<b>Constituents</b>	
Al <sub>2</sub> O <sub>3</sub>	20.20
Fe <sub>2</sub> O <sub>3</sub>	35.04
CaO	5.30
MgO	0.33
TiO <sub>2</sub>	4.00
Na <sub>2</sub> O	9.40
SiO <sub>2</sub>	17.29
Ignition	8.44
<b>Minerals(%)</b>	
Sodalite (Na <sub>2</sub> O.Al <sub>2</sub> O <sub>3</sub> .1,68SiO <sub>2</sub> .1,73H <sub>2</sub> O)	32.20
Cancrinite (3NaAlSiO <sub>4</sub> .NaOH)	4.60
Hematite (Fe <sub>2</sub> O <sub>3</sub> )	34.70
Diaspore (AlO(OH))	2.60
Rutile (TiO <sub>2</sub> )	1.60
Calcite (CaCO <sub>3</sub> )	1.30

The RM was thoroughly washed with distilled water until it became neutral. The suspension was wet sieved through a 200-mesh screen. A little amount of the suspension remained on the sieve and was discarded. The solid fraction was washed five times with distilled water following the sequence of mixing, settling and decanting. The last suspension was filtered, and the residual solid was then dried at 105°C, ground in a mortar and sieved through a 200-mesh sieve. Laccase from Russulaceae (*Lactarius volemus*) was purified by using precipitate of saturation (NH<sub>4</sub>)<sub>2</sub>SO<sub>4</sub>, DEAE-cellulose and immobilized on RM. 1 g of RM sample was shaken with 10 mL (5 µg protein/mL) laccase from *Lactarius volemus* solution for approximately 1 h and then the separated particles were stored. The laccase-modified RM was used for the study of AR37 dye removal from aqueous solution.

## 2.7 Material Characterization

The pH values were determined with a pH meter (Thermo scientific Orion 5 star plus multifunction). The scanning electron microscope (SEM) was used to examine the surface of the adsorbent. Images of native adsorbent and metal loaded adsorbent were magnified 5000 times by SEM modeled JEOL JSM-6400 SEM. Before SEM examinations, the sample surfaces were coated with a thin layer (20 nm) of gold to obtain a conductive surface and to avoid electrostatic charging during examination. The same machine was also used for the energy dispersive X-ray (EDX) spectra analysis to know the elemental composition of the RM. In addition, the Fourier Transform Infrared Spectroscopy (FTIR) analyses were carried out to identify functional groups and molecular structure in the laccase-modified RM and AR37 dye loaded laccase modified-RM. FTIR spectra were recorded on the on Perkin-a Perkin-Elmer GX2000 FTIR spectrometer. The spectrum of the adsorbent was measured within the range of 4000-700 cm<sup>-1</sup> wave number.

## 2.8 Adsorption Procedure

All experiments were performed at laboratory scale. Synthetic wastewater was prepared by dissolving AR37 dye in distilled water at 50 mg/L concentration (Fig. 1). All experimental procedures were done at 30°C and during 60 min. The AR37 adsorbed was determined using absorbance values measured before and after treatment, at 504 nm with PG Instruments T80 spectrophotometre. Calibration curves were established prior to the analysis. A calibration curve was prepared in the range 0-40 ngmL<sup>-1</sup> of AR37 dye according to the general procedure. The amounts of the dyes adsorbed onto compost ( $q_e$  in µg/g) and the percentages of the dyes removed from the solution ( $R$  in %) were calculated from the equations:

$$q_e = \frac{(C_o - C_e) * V}{m} \quad (1)$$

$$R = \frac{(C_o - C_t) * 100}{C_o} \quad (2)$$

where  $C_o$  and  $C_e$  are the initial and equilibrium concentrations of AR37 in solution (µg/L);  $V$  is the volume of solution (L) and  $m$  is the mass of adsorbent (g).

## 3. RESULTS AND DISCUSSION

### 3.1 Purification and Characterization of Laccase Enzyme from *Lactarius volemus*

A new laccase from the *Lactarius volemus* was purified and characterized by precipitating in (NH<sub>4</sub>)<sub>2</sub>SO<sub>4</sub> followed by anion-exchange and gel filtration chromatograph. ABTS was used as a substrate in the determination of activity in the protein eluted from the DEAE-sephadex column.

The results pertaining to purification of laccase using all purification techniques are summarized in Table 3. The final purification of 83.3-fold suggested that the laccase is highly abundant in the *Lactarius volemus*.

As shown in Fig. 2, SDS-PAGE revealed a single protein band at 20 kDa. The molecular weight of the enzyme was determined as 60 kDa by using the gel filtration chromatograph and comparing with known standard proteins. This result shown that purified laccase enzyme has three subunit.

**Table 3. The purification process of laccase from Russulaceae (*Lactarius volemus*)**

Enzyme fraction	Volume mL	Activity U/mL	Total Activity U	%	Protein (µg/ml)	Specific U/mg	Purification Fold
Crude extract	100	135.2±3.1	1.35x10 <sup>4</sup>	100	196.5±1.3	0.69	-
(NH <sub>4</sub> ) <sub>2</sub> SO <sub>4</sub>	80	88.3±1.2	7.1 x10 <sup>3</sup>	52.6	47.2±2.2	1.87	2.7
DEAE-sephadex	50	73.1±0.3	3.76	27.9	4.53±1.3	16.13	23.4
Sephacryl S 200	30	63.2±1.1	1.9 x10 <sup>3</sup>	14.1	1.10±1.5	57.5	83.3

## 3.2 Characterization Study

### 3.2.1 FT-IR

The FT-IR can provide very useful information about functional group. The technique can be used to analyze organic materials and some of inorganic materials. The FT-IR technique is to measure the absorption of various infrared radiations by the target material, to an IR spectrum that can be used to identify functional groups and molecular structure in the sample. The functional groups and surface properties of the adsorbent after adsorption by FT-IR spectra were illustrated in Fig. 3.

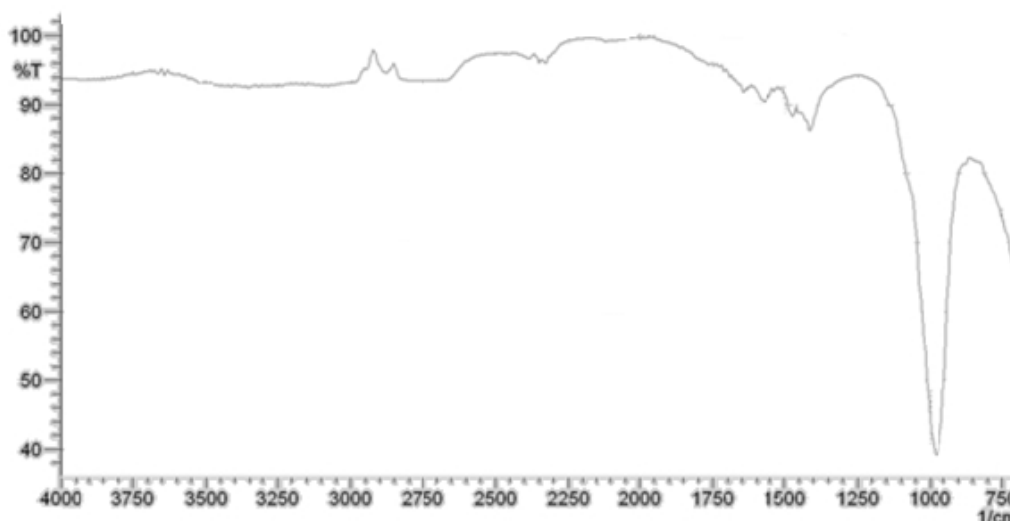


**Fig. 3. FT-IR spectrum of adsorbent loaded with copper ions.**

At 3262-3269  $\text{cm}^{-1}$ , a strong band was present in the hydroxyl stretching region in the spectra. This was likely due to the presence of  $\text{H}_2\text{O}$  in the red mud [51,52]. At 1644  $\text{cm}^{-1}$ , a band was detected. This was attributed to the water molecules occluded inside the aluminosilicate structure [53]. The absorption band of carbonates incorporated in the main channel of cancrinite [54], appeared within the 1410-1470  $\text{cm}^{-1}$  region in the samples. The peak recorded at 1410  $\text{cm}^{-1}$  in the samples could be attributed to  $\text{NO}_3^-$  present in both cancrinite and sodalite. The band at 964-970  $\text{cm}^{-1}$  observed in samples could be assigned to the stretching vibrations of  $\text{Si(Al)-O}$ . This band is sensitive to the content of structural Si and Al. To evaluate, through the FTIR technique, the interaction mechanisms between the AR37 ions and RM, we focused our attention on a part of the midinfrared region, 687-862  $\text{cm}^{-1}$ , where bands associated with various AR37-O(H) stretching vibrations were found [55]. It is shown that there is no significant change in the functional biomass groups of clay soil after adsorption of AR37 ions on the red mud when AR37 ions were treated with red mud. It was concluded that AR37 dye did not damage to functional groups on the adsorbent.

### 3.2.2 SEM study

SEM has been a primary tool for characterizing the surface morphology and fundamental physical properties of the adsorbent surface. It is useful for determining the particle shape,



porosity and appropriate size distribution of the adsorbent [56]. SEM of RM and AR37 dye adsorbed laccase modified-RM are shown in Fig. 4. It is clear that, RM has considerable numbers of pores where, there is a good possibility for dyes to be trapped and adsorbed into these pores. Based on analysis of the images taken by SEM before and after the dye adsorption process, highly heterogeneous pores within RM particles were observed. After AR37 dye adsorption, the pores were packed with dyes.

### **3.2.3 EDX study**

The EDX measurements were recorded for qualitative analysis of the element constitution of the adsorbents and the EDX spectra of native adsorbent and AR37 dye loaded adsorbent were illustrated in the Fig. 5a and b. From the EDX spectra, the AR37 dye ions were adsorbed onto the laccase modified-RM adsorbent. It is shown from EDX spectra that after AR37 dye adsorption, element concentrations increased in the AR37 dye loaded adsorbent (Table 4).

**Table 4. Results of EDX spectrum**

Elements	Native adsorbent (RM)		AR37 dye loaded adsorbent (Laccase modified-RM)	
	Weight (%)	Atom (%)	Weight (%)	Atom (%)
Na	14.00	21.49	11.29	18.44
Si	15.58	19.59	10.43	13.94
Al	20.02	26.19	17.25	24.00
K	0.66	0.60	1.01	0.97
Ca	1.00	0.88	3.18	2.98
Ti	5.21	3.84	7.70	6.03
Fe	42.29	26.73	47.60	32.00
Cu	1.24	0.69	1.55	1.64

## **3.3 Adsorption Study**

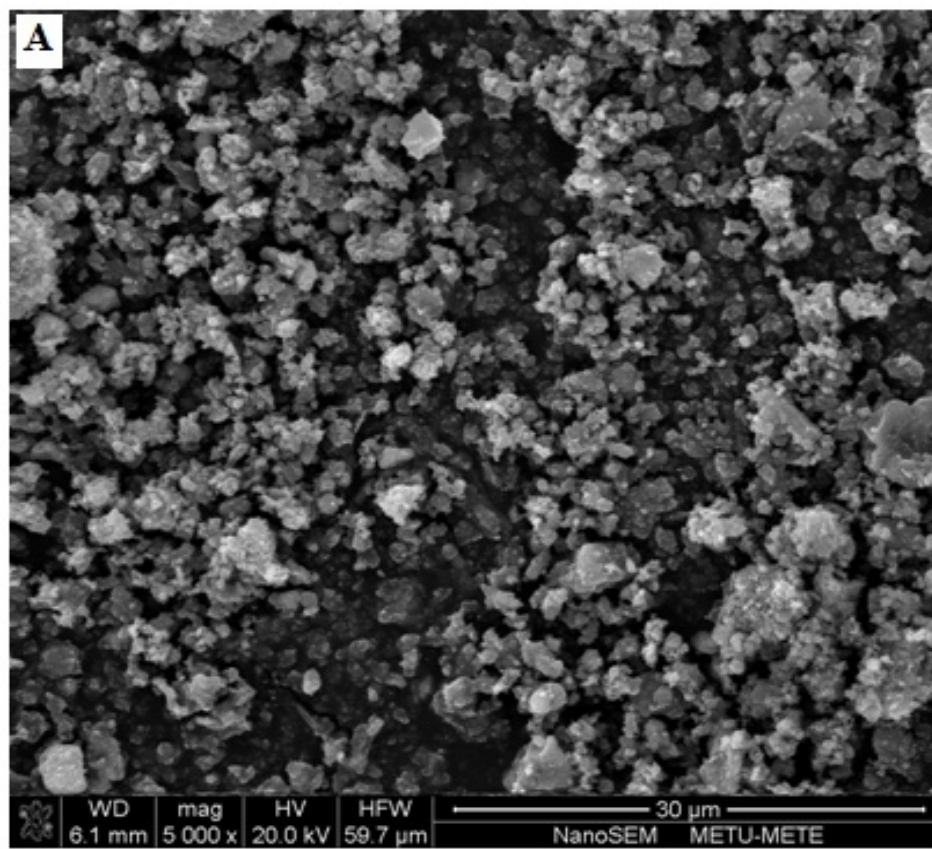
### **3.3.1 Effect of pH**

One of the most important factors affecting the capacity of adsorbents in wastewater treatment is pH [57]. The pH of the solution affects the surface charge of the adsorbents as well as the degree of ionization of different pollutants. The hydrogen ion and hydroxyl ions are adsorbed quite strongly and therefore the adsorption of other ions is affected by the pH of the solution. Change of pH affects the adsorptive process through dissociation of functional groups on the adsorbent surface active sites [58]. The effect of the initial pH of the dye solution towards the adsorption of AR37 by laccase modified- RM in dye solution is shown in the Fig. 6. In order to evaluate the influence of pH on the adsorption, the experiments were carried out at different initial pH values ranging from 3 to 9. The optimum pH, at which the maximum removal occurred, was obtained as 4. At lower pH values, the amount of dye adsorbed decreased due to repulsive force between positively charged surface and the positively charged dyes molecules [59]. At lower pH more protons will be available, thereby increasing electrostatic attractions between negatively charged dye anions and positively charged adsorption sites and causing an increase in dye adsorption. When the pH of the solution is increased, the positive charge on the oxide or solution interface decreases and the adsorbent surface becomes negatively charged. The adsorbent surface

metal binding sites as well as dye chemistry in solution were influenced by solution pH. It is to be expected that with increase in pH values, more and more ligands having negative charge would be exposed which result in increase in attraction of positively charged dye ions.

### 3.4 Effect of Contact Time

The contact time is inevitably a fundamental parameter in all transfer phenomena such as adsorption [60]. Therefore, it is important to study its effect on the capacity of retention of AR37 dye by laccasa modified-RM. The effect of contact time on removal of the dye is shown in Fig. 7. The removal increased quickly within the initial 25 min and remained almost unchanged after 60 min, indicating reaching an apparent equilibrium. Rapid absorption and equilibrium in a short period of time is related to the efficacy of the adsorbent, especially for wastewater treatment [61-63]. The amount of the removal increased with the increase of the contact time and reached a constant value. This may be due to the attainment of equilibrium condition at 30 min of contact time, which is fixed as the optimum contact time. At the initial stage, the rate of the removal of AR37 was higher, due to the availability of more than required number of active sites on the surface of adsorbent. The rate of the removal became slower at the later stages of contact time, due to the decreased or lesser number of active sites [64,65].



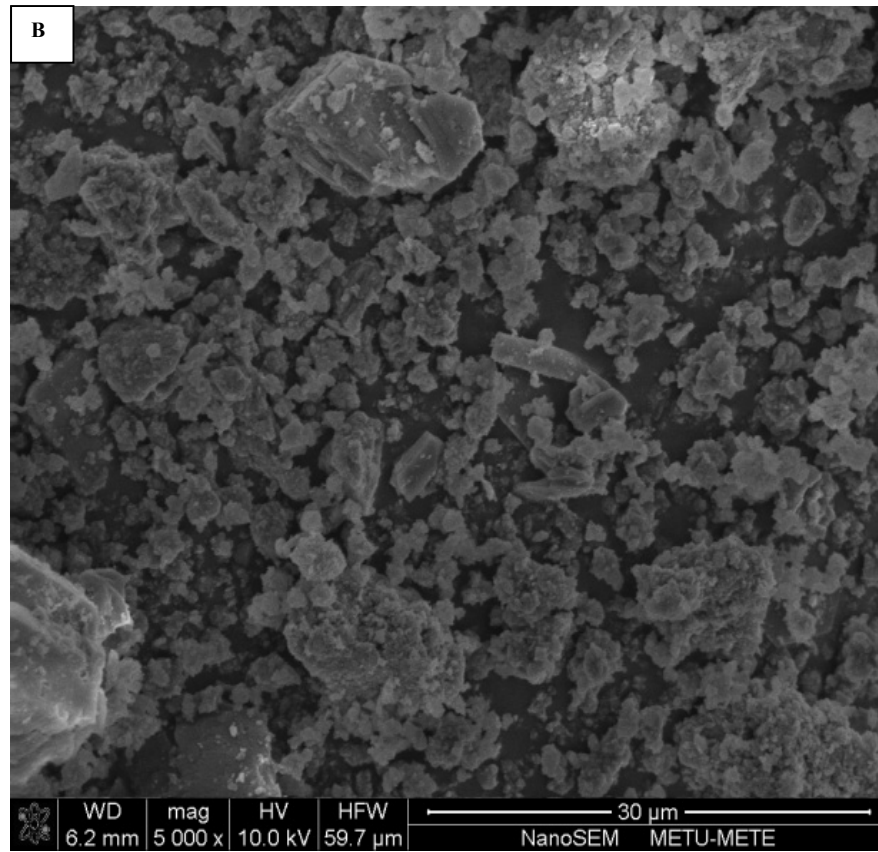
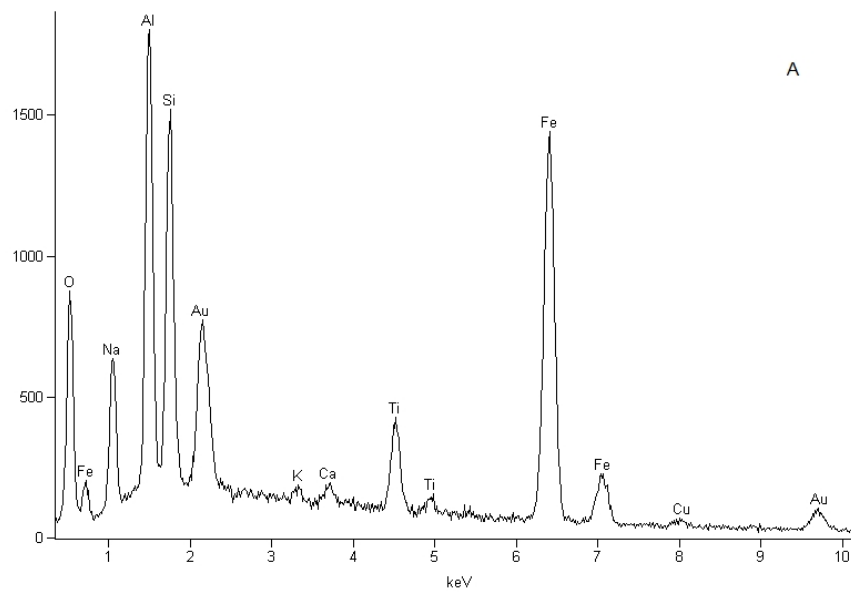


Fig. 4. SEM images of native RM (A) and AR37 dye loaded laccase modified-RM (B).



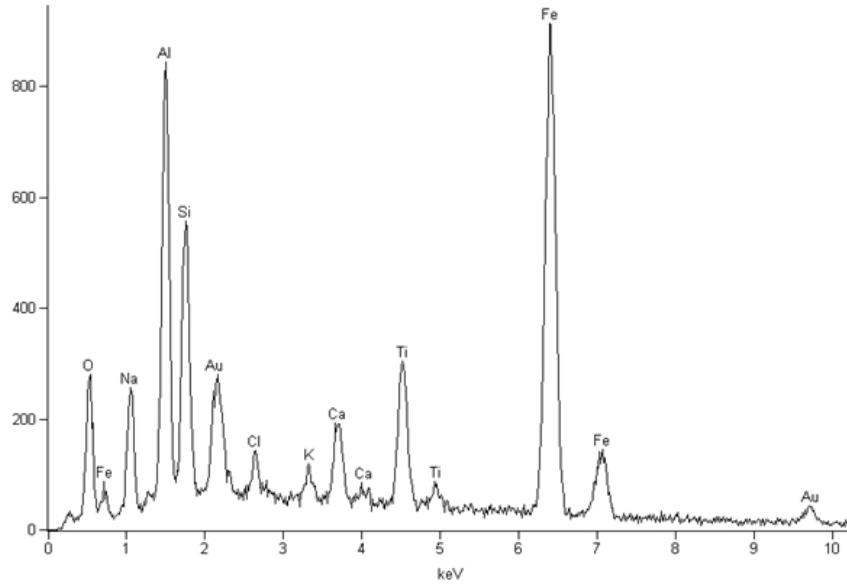


Fig. 5. EDX spectra of native RM (A) and AR37 dye loaded laccase-modified RM (B).

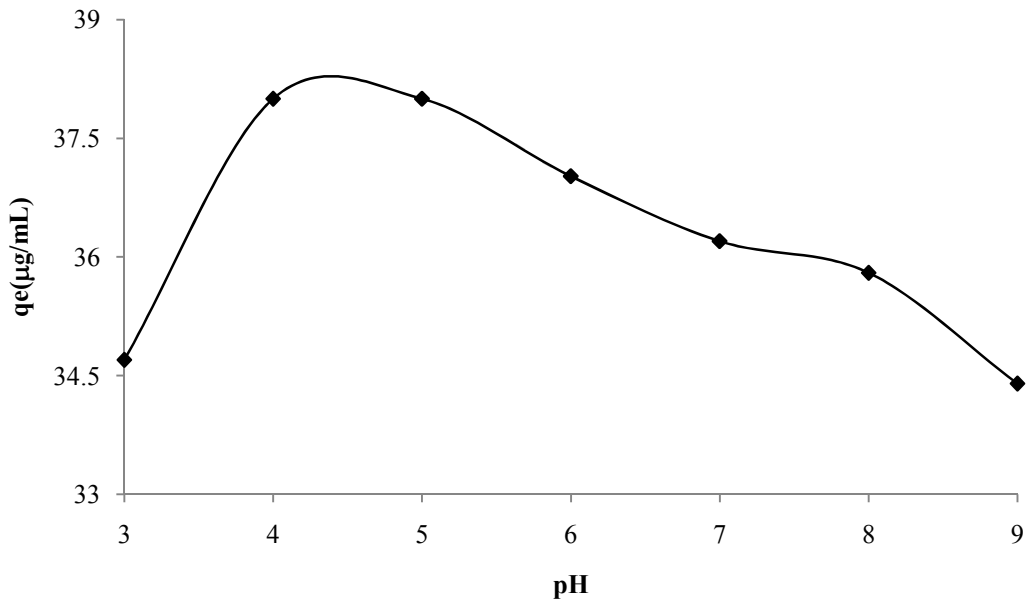
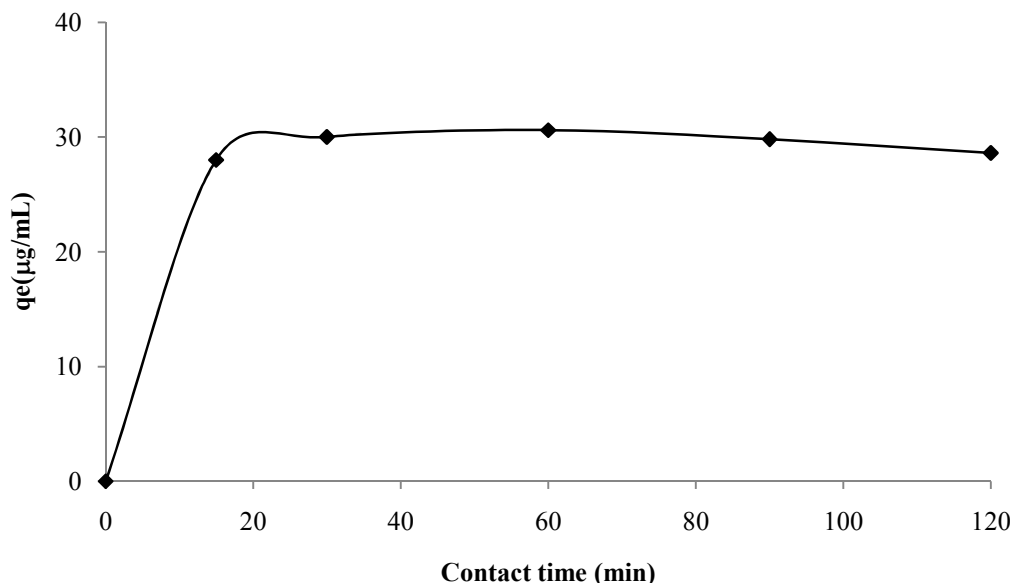


Fig. 6. Effect of pH on the removal of AR37 dye by laccase-modified RM.



**Fig. 7. Effect of contact time on the removal of AR37 by laccase-modified RM.**

### 3.5 Effect of Temperature

Temperature known to have a profound effect on various chemical processes is one of the most important controlling parameter in adsorption. It affects the adsorption rate by altering molecular interactions and solubility of adsorbate [66-68]. The effect of temperature was investigated in the temperature range 20 to 80°C (Fig. 8). It was observed that the removal of AR37 dye increased from 29.96 to 34.96  $\mu\text{g/g}$  by increasing the temperature from 20 to 30°C. This increase in adsorption is mainly due to increase in number of adsorption sites caused by breaking of some of the internal bonds near the edge of the active surface sites of the adsorbents [67]. This phenomenon also leads to an increment in the availability of active surface sites, increased porosity and in the total pore volume of the adsorbent. However, the adsorption capacity slightly decreased from 34.96 to 29.22  $\mu\text{g/g}$  with increasing the temperature from 30°C to 80°C. This may be attributed by the fact that the mobility of the dye molecule increases with increasing the temperature, which may responsible for the decrease of adsorption capacity of adsorbent. The similar result was reported in the previous study [69-71].

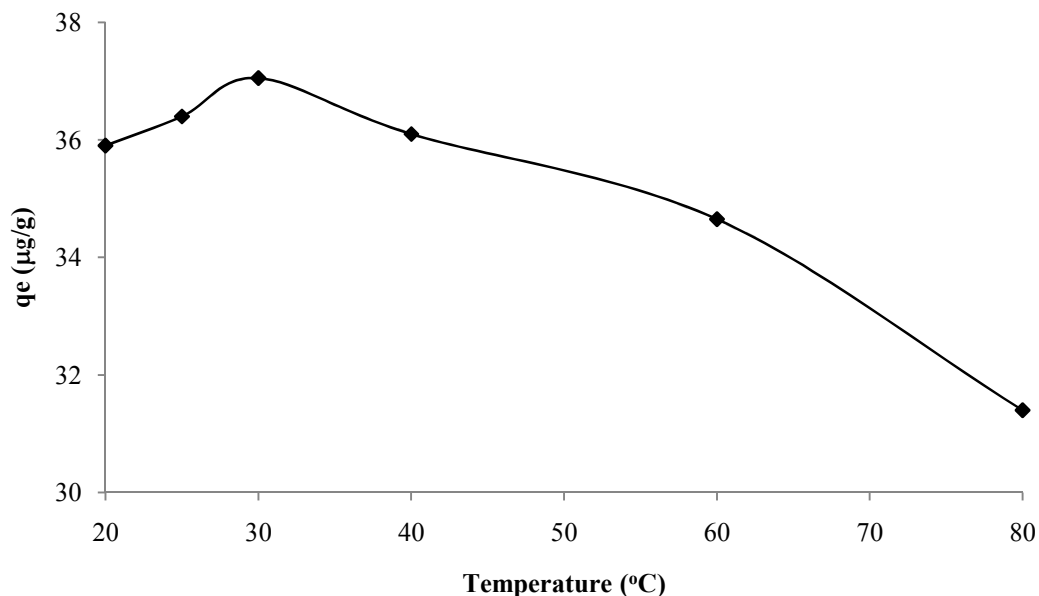


**Fig. 8. Effect of temperature on the removal of AR37 dye by laccase-modified RM.**

### 3.6 Effect of Adsorbent Dosage

Dosage study is an important parameter in adsorption studies because it determines the capacity of adsorbent for a given initial concentration of dye solution [65]. The effect of the adsorbent dosage was studied by varying the adsorbent amounts from 0.125 to 2.0 mg/mL. The effect of laccase modified-RM dosage on amount of AR37 dye adsorbed was shown in Fig. 9. A trend of increase in adsorption capacity with increase in adsorbent dosage was observed from 0.125 to 1 mg/mL. Any further addition of the adsorbent beyond this did not cause any significant change in the adsorption. The amount of maximum AR37 dye removal was 55.12 µg/g at 1 mg/mL of adsorbent dose. Increase in adsorbent dosage increased the percent removal of dye, which is due to the increase in adsorbent surface area of the adsorbent [72]. Increase in adsorption with increase in adsorbent dosage attributed to the increase of active sites for adsorption of dye molecules with increasing adsorbent dosage. At very low adsorbent concentration, the adsorbent surface becomes saturated with the dye and the residual dye concentration in the solution to large [65].

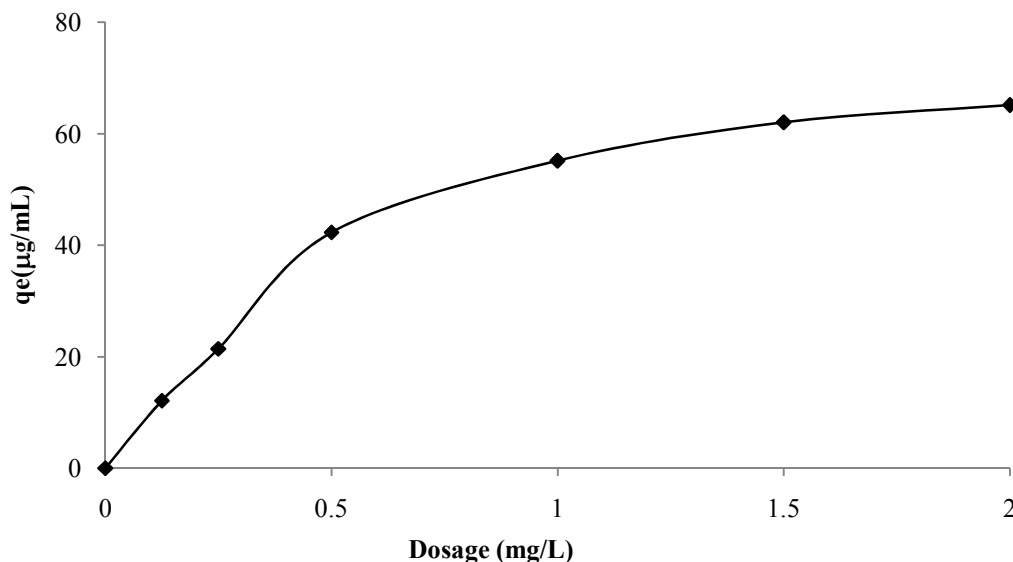


Fig. 9. Effect of adsorbent dosage on removal of AR37 by laccase-modified RM.

### 3.7 Equilibrium Adsorption Isotherms

The relationship between the amounts a substance adsorbed at constant temperature and its concentration in the equilibrium solution is called the adsorption isotherm. The adsorbent isotherm is important from both theoretical and practical point of view [72]. In order to optimize the design of an adsorption system to remove dye from solutions, it is important to establish the most appropriate correlation for the equilibrium curve. Therefore, the two well-known and widely applied isotherm equations, namely the Langmuir and Freundlich models, were applied to determine the experimental data. There are different equation parameters and the underlying thermodynamic presuppositions of these models often provide insight into both adsorption mechanism and surface properties of the adsorbents [42,73,74]. The suitability of the Langmuir and Freundlich adsorption isotherm models to the equilibrium data was investigated and the Langmuir and Freundlich isotherm constants for the AR37 adsorption on the laccase modified-RM were determined.

The Langmuir adsorption isotherm is often used to describe the maximum adsorption capacity of an adsorbent and it is given as;

$$q_e = \frac{q_{max} * b * C_e}{1 + b * C_e} \quad (3)$$

where  $q_{max}$  ( $\mu\text{g/g}$ ) and  $b$  ( $\text{L/mg}$ ) are Langmuir constants which are indicators of the maximum adsorption capacity and the affinity of the binding sites, respectively. They can be determined from a linear form of Eq. 2 (by plotting the  $C_e/q_e$ ) versus  $C_e$ , represented by calculated with the following equation;

$$\frac{C_e}{q_e} = \frac{1}{b * q_{max}} + \frac{C_e}{q_{max}} \tag{4}$$

The values of  $q_{max}$  and  $b$  were calculated from the slope and intercept of the Langmuir plot of  $C_e$  versus  $C_e/q_e$  from Fig. 10, the empirical constants  $q_{max}$  and  $b$  were found to be 0.4412 mg/g and 0.0049 L/mg (Table 5), respectively. The correlation coefficient reported in Table 5 showed strong positive evidence on the adsorption of AR37 onto laccase modified-RM follows the Langmuir isotherm. The applicability of the linear form of Langmuir model to laccase modified-RM was proved by the high correlation coefficient  $R^2$  (0.99) > 0.95. This suggests that the Langmuir isotherm provides a good model of the sorption system.

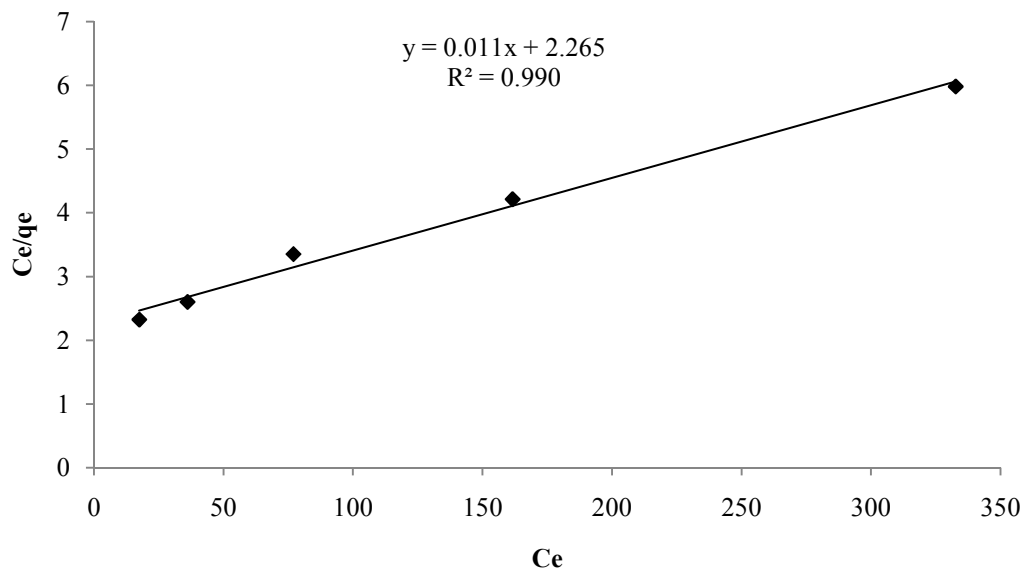


Fig. 10. Langmuir adsorption isotherm.

Table 5. Values of the Langmuir and Freundlich adsorption isotherms

Adsorption isotherm	Value
<i>Langmuir constants</i>	
$q_{max}$ (mg/g)	0.4412
$b$ (L/mg)	0.00489
$R^2$	0.990
<i>Freundlich constants</i>	
$K_F$	0.87
$n$	0.691
$R^2$	0.996

The Freundlich isotherm model is an empirical relationship describing the adsorption of solutes from a liquid to a solid surface and assumes that different sites with several adsorption energies are involved [75]. It is described by the following equation;



$$q_{\max} = K_F C_e^{1/n} \quad (5)$$

where  $K_F$  and  $n$  are the Freundlich constants related to the sorption capacity of the adsorbent ( $\mu\text{g/g}$ ) and the energy of adsorption, respectively. They can be calculated in the following linear form;

$$\log q_e = \log K_F + \frac{1}{n} \log C_e \quad (6)$$

$K_F$  and  $n$  values were calculated from the intercept and slope of the plot (Fig. 11). In the literature, it is pointed out that the parameters,  $K_F$  and  $n$  affect the adsorption isotherm. The larger  $K_F$  and  $n$  values indicate the higher the adsorption capacity. The magnitude of exponent  $n$  gives an indication of the favorability of the adsorption. The  $n$  value is 0.74 (Table 5) and it is good adsorption characteristic [76]. Based on the high correlation coefficient  $R^2$  (0.9892)  $>$  0.95, it has been deduced that Freundlich model better fitted to the experimental data (Table 5). The high correlation coefficient showed that both adsorption isotherm models are suitable for describing the adsorption equilibrium of AR37 dye.

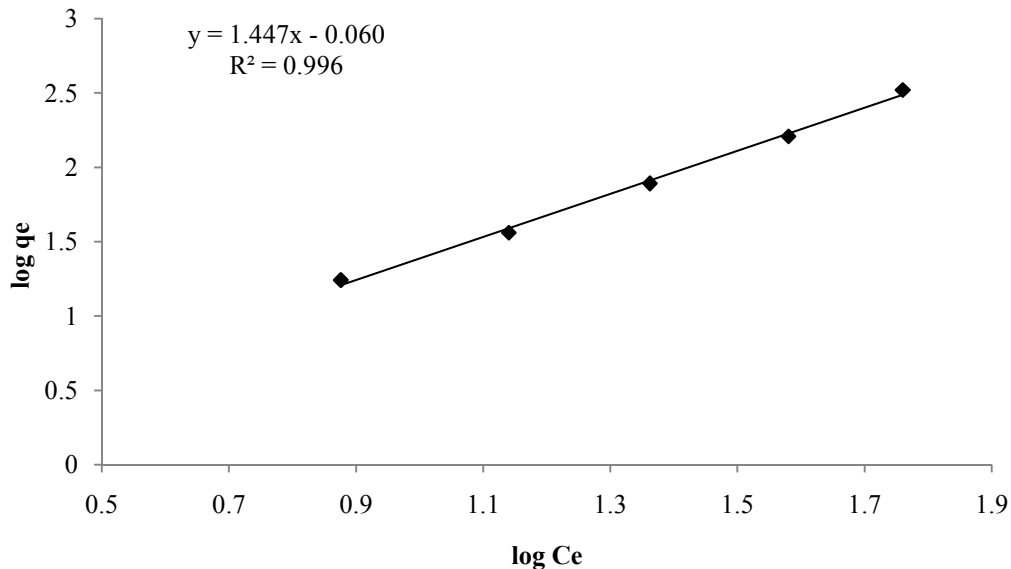


**Fig. 11. Freundlich adsorption isotherm.**

To understand the mechanisms and dynamics of the adsorption process, the pseudo-first-order kinetic and pseudo-second-order kinetic models were used to evaluate the experimental data, which were generated through the AR37 adsorption tests using the laccase-modified red mud. The following Lagergren kinetic equation, which is known as the pseudo-first-order kinetic model, is used widely to understand the kinetic behavior specific to adsorption reactions

$$1/q_t = k_1/q_e t + 1/q_e \quad (7)$$

where  $k_1$  is the pseudo-first-order rate constant ( $\text{min}^{-1}$ ),  $q_e$  and  $q_t$  are the amounts of AR37 adsorbed at time  $t$  and at equilibrium ( $\mu\text{g/g}$ ). This equation has been applied to the current study on AR37 adsorption. At different concentrations from 5 to 100  $\mu\text{g/L}$ , the correlation coefficients and  $k_1$  were calculated for AR37 adsorption from the linear plots of  $\log(q_e - q_t)$  vs.  $t$  (Fig. 12), and shown in Table 4. Pseudo-first-order kinetic model's correlation coefficients were high at ranges 0.976 to 0.9978. Besides, there were a great difference between experimental and calculated equilibrium adsorption capacities ( $q_e$ ), which suggests a higher pseudo first-order fit on the experimental data. These findings confirm laccase-modified red mud's increased adsorption capacity.

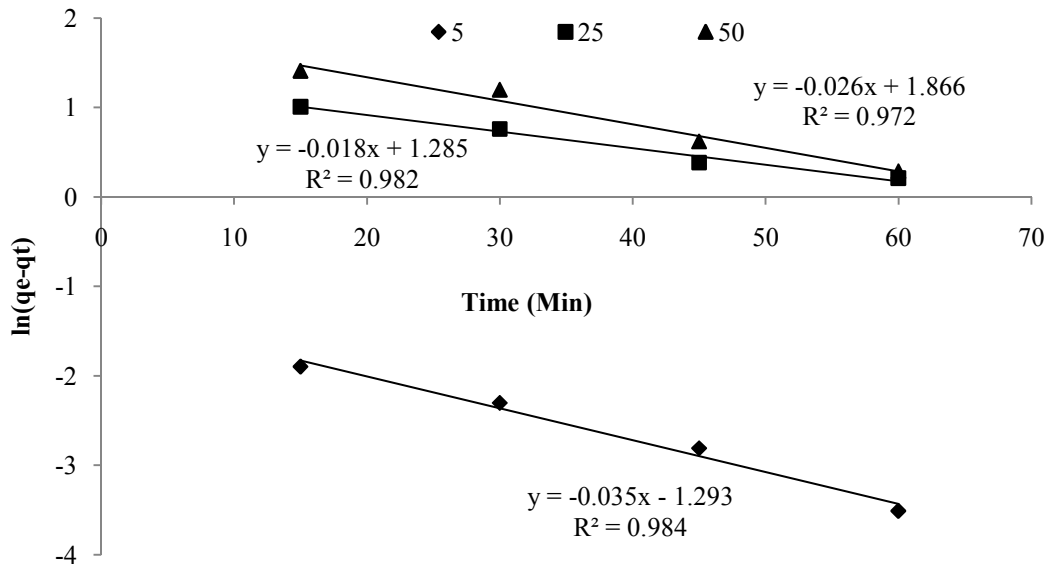


**Fig. 12. Pseudo first-order reaction for AR37 adsorbed onto red mud adsorbent at different concentrations.**

It is also possible to describe the adsorption kinetics by a pseudo-second order reaction. Pseudo-second-order kinetic model assumes that chemisorption may be the limiting rate step, where the valence forces are involved between the adsorbent and adsorbate, through electron sharing or Exchange [77]. Equation for the pseudo-second-order kinetic model is as follows.

$$1/q_t = k_2/q_e^2 + t/q_e \tag{8}$$

where, the equilibrium rate constant of pseudo-second-order model is  $k_2$  here ( $\text{g mol}^{-1} \text{min}^{-1}$ ). This equation has been applied to the current study on AR37 adsorption. At different concentrations from 5 to 50  $\mu\text{g/L}$ , the correlation coefficients,  $q_e$  and  $k_1$  were calculated for AR37 adsorption from the linear plots of  $t/q_t$  vs.  $t$  (Fig. 13) and shown in Table 6. Straight lines with high correlation coefficients ( $>0.9570$ ) were obtained for all the initial AR37 concentrations studied. Besides, experimental data also agree with the calculated  $q_e$  values, in terms of the pseudo-second-order kinetics.

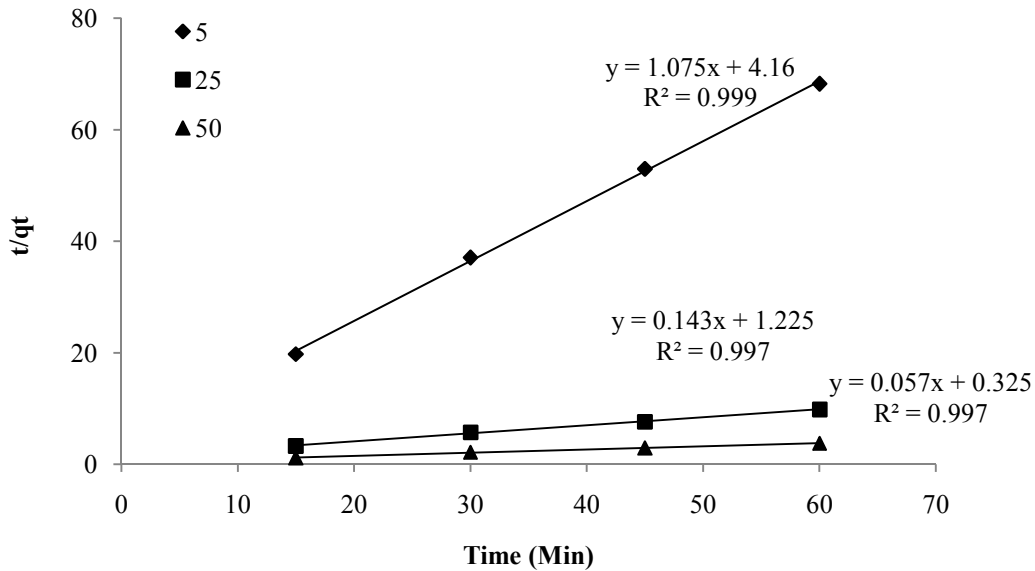


**Fig. 13. Pseudo second-order reaction for AR37 adsorbed onto laccase-modified RM adsorbent at different concentrations.**

**Table 6. Comparison between the estimated adsorption rate constants,  $q_e$  and correlation coefficients associated with the pseudo-first-order and the pseudo-second-order rate equations**

Initial AR37 concentration ( $\mu\text{g/L}$ )	Pseudo-first-order rate equation				Pseudo-second-order rate equation		
	$q_e, \text{exp}$ ( $\mu\text{g/g}$ )	$k_1$	$q_e, \text{cal}$ ( $\mu\text{g/g}$ )	$R^2$	$k_2$	$q_e, \text{cal}$ ( $\mu\text{g/g}$ )	$R^2$
5	1.19	0,026	6,46	0,972	0,29	0.93	0,999
25	13.36	0,018	3,61	0,982	0,015	6.99	0,997
50	27,43	0,035	0,274	0,984	0,01	17.54	0,997

This pseudo-second-order kinetic analysis suggests that as the initial AR37 concentration increases  $k_2$  decreases. Probably, this behavior is caused by the lower competition for the sorption surface areas, at lower concentrations. At higher concentrations, however, lower sorption rates are obtained as the competition for the surface active sites is higher. On the other hand, equilibrium adsorption capacity ( $q_e$ ) increases as the initial AR37 concentration increase, since most of the AR37 ions are adsorbed at available adsorption sites [75].

### 3.8 Adsorption Thermodynamic

In environmental engineering practice, both energy and entropy consideration must be taken into account in order to determine what processes will occur spontaneously [78]. The aim of thermodynamic study is to establish the thermodynamic parameters that can characterize the adsorption process of AR37 dye onto laccase modified-RM. The adsorption capacity of laccase modified-RM adsorbent increased with increase in the temperature of the system from 293-303 K. Thermodynamic parameters such as change in free energy ( $\Delta G^\circ$ ) kJ/mol,

enthalpy ( $\Delta H^\circ$ ) kJ/ mol and entropy ( $\Delta S^\circ$ ) J/Kmol were determined using the following equations [79]:

$$K_L = \frac{C_s}{C_e} \quad (7)$$

$$\Delta G^\circ = -RT \ln K_L \quad (8)$$

$$\ln K_L = \left(\frac{\Delta S^\circ}{R}\right) - \left(\frac{\Delta H^\circ}{RT}\right) \quad (9)$$

where  $K_L$  is the equilibrium constant,  $C_s$  is the solid phase concentration at equilibrium ( $\mu\text{g/L}$ ),  $C_e$  is the liquid phase concentration at equilibrium ( $\mu\text{g/L}$ ),  $T$  is the temperature in Kelvin and  $R$  is the gas constant.

$\Delta H^\circ$  and  $\Delta S^\circ$  values are obtained from the slope and intercept of plot  $\ln K_o$  against  $1/T$  [80]. Von't Hoff plot of effect of temperature on adsorption of AR37 on laccase modified-RM was illustrate on Fig. 14 and the observed thermodynamic values were summarized in Table 7 [81,82].

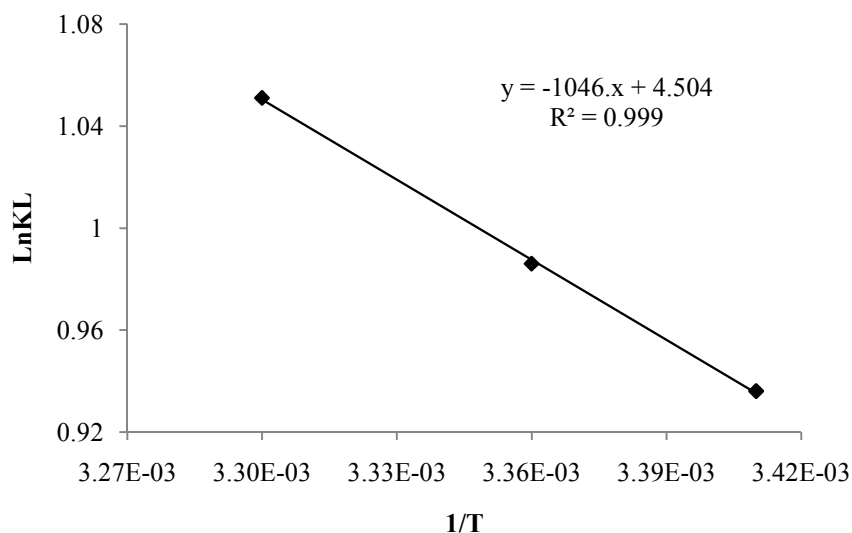


**Fig. 14. Influence of temperature on the thermodynamic behavior of AR37 dye.**

The negative value of  $\Delta G^\circ$  indicates the adsorption is favorable and spontaneous. The  $\Delta G^\circ$  values decrease with an increase in temperature, indicating an increased trend in the degree of spontaneity and feasibility of AR37 dye adsorption. The negative values of  $\Delta H^\circ$  further confirm the exothermic nature of adsorption process. Hence, the adsorption of AR37 dye on laccase modified-RM is chemical in nature. The positive values of  $\Delta S^\circ$  indicate the increased disorder and randomness at the solid solution interface of AR37 dye with the adsorbent.

**Table 7. Thermodynamic parameters for the AR37 dye adsorption**

Temperature (K)	Thermodynamic parameters		
	$\Delta G^\circ$ (kJmol <sup>-1</sup> )	$\Delta H^\circ$ (kJmol <sup>-1</sup> )	$\Delta S^\circ$ (Jmol <sup>-1</sup> )
298	-9.37	-85.77	0.37
303	-14.44		
313	-21.02		

#### 4. CONCLUSION

In this study, RM modified using laccase from Russulaceae (*Lactarius volemus*) was converted into an adsorbent and the suitability of the activated RM for adsorption of AR37 dye from textile wastewater was investigated. The results indicate that laccase modified-RM can be successfully used for the adsorption of AR37 from aqueous solutions. The pH, biosorbent dose, time, initial dye concentration and temperature affected the adsorption process. The optimum pH for efficient adsorption of AR37 is 4. The adsorption capacity is strongly dependent on the temperature and increases significantly with increase in temperature from 20 to 30°C. For equilibrium studies, two isotherm models were used in this study, which is Freundlich and Langmuir, for different temperatures and it is found that Freundlich fitted experimental data very well. Thermodynamic parameters including the Gibbs free energy, enthalpy and entropy changes indicated that the adsorption of AR37 onto laccase modified-RM adsorbent was feasible, spontaneous and exothermic. Based on the results, laccase modified-RM can be used as a relatively efficient and low cost adsorbent for the removal of AR37 dye from textile wastewater.

#### COMPETING INTERESTS

Authors have declared that no competing interests exist.

#### REFERENCES

1. Leshem EN, Pines DS, Ergas SJ, Rechow DA Electrochemical oxidation and oxidation for textile wastewater reuse. *J Env Eng.* 2006;132:324-330.
2. Aleboye A, Daneshvar N, Kasiri MB. Optimization of Cl acid red 14 azo dye removal by electrocoagulation batch process with response surface methodology. *Chem Eng Process.* 2008;47:827-832.
3. Bandala ER, Pelaez MA, Garcia AJ, Salgado MJ, Moeller G. Photocatalytic decolorization of synthetic and real textile wastewater containing benzidinebased azo dyes. *Chem Eng Process.* 2008;47:69-176.
4. Orozco SL, Bandala Er, Arancibia-Bulnes CA, Serrano B, Suarez-Parra R, Hernandez-Perez I. Effect of iron salt on the color removal of water containing the azo-dye reactive Blue 69 using photo-assisted Fe(II)/H<sub>2</sub>O<sub>2</sub> and Fe(III)/H<sub>2</sub>O<sub>2</sub> systems. *J Photoch Photobio A: Chem.* 2008;198:144-149.
5. Puvaneswari N, Muthukrishnan J, Gunasekaran P. Toxicity Assessment and microbial degradation of azo dyes. *Indian J Exp Biol.* 2006;44:618-626.
6. Karimi A, Vahabzadeh F, Mohseni M, Mehranian M. Decolorization of maxilon-red by kissiris immobilized phanerochaete chrysosporium in a trickle-bed bioreactor-involvement of ligninolytic enzymes *Iranian J Chem Chem Eng.* 2009;28(3):1-13.

7. Shokoohi R, Vatanpoor V, Zarrabi M, Vatani A. Adsorption of acid red 18 (AR18) by activated carbon from poplar wood: kinetic and equilibrium study. *E-J Chem.* 2010;7:65-72.
8. Samarghandi MR, Zarrabi M, Sepehr NM, Panahi R, Foroghi M. Removal of acid red 14 by pumice stone as a low cost adsorbent: Kinetic and equilibrium study. *Iranian J Chem Eng*, 2012;31(3):19-27.
9. Tan NCG, Borger A, Slenders P, Svitelskaya A, Lettinga G, Field JA. Degradation of azo dye mordant yellow 10 in a sequential anaerobic and bioaugmented aerobic bioreactor *Water Sci Technol.* 2000;42(5-6):337-344.
10. Kalyuzhnyi S, Sklyar V. Biomineralisation of azo dyes and their breakdown products in anaerobic-aerobic hybrid and UASB reactors. *Water Sci Technol.* 2000;41(12):23-30.
11. O'Neill C, Lopez A, Esteves S, Hawkes FR, Hawkes DL, Wilcox S. Azo-dye degradation in an anaerobic-aerobic treatment system operating on simulated textile effluent. *Appl Microbiol Biot.* 2000;53(2):249-254.
12. Dos Santos AB, Bisschops IAE, Cervantes FJ, van Lier JB. Effect of different redox mediators during thermophilic azo dye reduction by anaerobic granular sludge and comparative study between mesophilic (30°C) and thermophilic (55°C) treatments for decolourisation of textile wastewaters *Chemosphere*, 2004;55:1149-1157.
13. Yilmaz A, Yilmaz E, Yilmaz M, Bartsch RA. Removal of azo dyes from aqueous solutions using calix[4]arene and B-Cyclodextrin. *Dyes and Pigments.* 2007;74:54-59.
14. Ertugrul S, San, NO Donmez G. Treatment of dye (remazol blue) and heavy metals using yeast cells with the purpose of managing polluted textile wastewaters *Ecol Eng.* 2009;35:128-134.
15. Mohan SV, Rao CN, Sarma PN. Simulated acid azo dye (acid black 210) wastewater treatment by periodic discontinuous batch mode operation under anoxic-aerobic-anoxic microenvironment conditions. *Ecol Eng.* 2007;31:242-250.
16. Garg VK, Gupta R, Yadav AB, Kumar R. Dye removal from aqueous solution by adsorption on treated sawdust *Bioresource Technol.* 2003;89:121-124.
17. Robinson T, Chandran B, Nigam P. Removal of dyes from a synthetic textile dye effluent by biosorption on apple pomace and wheat straw. *Water Res.* 2002;36:2824-2830.
18. Nadaroglu H, Kalkan E, Demir N. Removal of copper from aqueous solution using red mud *Desalination*, 2010;153:90-95.
19. Nadaroglu H, Kalkan E. Alternative absorbent industrial red mud waste material for cobalt removal from aqueous solution. *Inter J Phy Sci*, 2012;7(9):1386-1394.
20. Nadaroglu H, Celebi N, Kalkan E, Dikbas N. The Evaluation of affection of *methylobacterium extorquens* -modified silica fume for adsorption cadmium (II) ions from aqueous solutions affection. *J FacVet Med Kafkas Univ.* 2013;19(3):391-397.
21. Mane RS, Bhusari VN. Removal of colour (dyes) from textile effluent by adsorption using orange and banana peel. *Int J Chem Eng Appl.* 2012; 2(3):997-2004.
22. Ngah WSW, Hanafiah MAKM. Removal of heavy metal ions from wastewater by chemically modified plant wastes as adsorbents: A review *Biores Technol.* 2008;99:3935-3948.
23. Sivaraj R, Namasivayam C, Kadirvelu K. Orange peel as an adsorbent in the removal of acid violet 17 (acid dye) from aqueous solutions. *Waste Manage.* 2001;21(1):105-110.
24. Wang S, Zhu ZH. Sonochemical treatment of fly ash for dye removal from wastewater. *J Hazard Mat B.* 2005;126:91-95.
25. Mane VS, Mall ID, Srivastava VC. Kinetic and Equilibrium isotherm studies for the adsorptive removal of brilliant green dye from aqueous solution by rice husk ash. *J Env Manag.* 2007;84:390-400.

26. Dincer AR, Gunes Y, Karakaya N, Gunes E. Comparison of activated carbon and bottom ash for removal of reactive dye from aqueous solution. *Bioresource Technology* 2007;98:834-839.
27. Namasivayam C, Kavitha D. Removal of congo red from water by adsorption onto activated carbon prepared from coir pith, an agricultural solid waste. *Dyes Pigments*. 2002;54:47-58.
28. Nadaroglu H, Celebi N, Kalkan E, Tozsın G. Water purification of textile dye acid red 37 adsorption on laccase-modified silica fume. *Jökull J.* 2013; 63 (5): 87-113.
29. Kalkan E, Nadaroglu H, Celebi N, Tozsın G. Removal of textile dye reactive black 37 from aqueous solution by adsorption on laccase-modified silica fume. *Desalination And Water Treatment* (in press); 2013.
30. Ozdemir O, Armagan B, Turan M, Celik MS. Comparison of the adsorption characteristics of azo- reactive dyes on mesoporous minerals. *Dyes Pigments*. 2004;62:49-60.
31. Gong R, Ding Y, Li M, Yang C, Liu H, Sun Y. Utilization of powdered peanut hull as biosorbent for removal of anionic dyes from aqueous solution. *Dyes Pigments*. 2005;64:187-192.
32. Rachakornkij M, Ruangchuay and S Teachakulwiroj S Removal of reactive dyes from aqueous solution using bagasse fly ash. *Songklanakarin J Sci Technol.* 2004;26:13-24.
33. Ponnusami V, Kritika V, Madhuram R, Srivastava SN Biosorption of reactive dye using acid-treated rice husk: factorial design analysis. *J Hazard Mat.* 2007;142:397-403.
34. Chvedov D, Ospat S, Le T Surface properties of red mud particles from potentiometric titration *Colloids and Surfaces A.* 2001;182(2):131-141.
35. Garcia-Sanchez A, Alvarez-Ayuso E. Sorption of Zn, Cd and Cr on calcite application to purification of industrial wastewaters. *Mineral Eng.* 2002;15:539-547.
36. Gupta VK, Ali I, Saini VK. Removal of chlorophenols from wastewater using red mud: an aluminum industry waste. *Env Scid Tech.* 2004;38:4012-4018.
37. Tian X, Wu B, Li J. The Exploration of making acid proof fracturing proppants using red mud. *J Hazard Mat.* 2008;160:589-593.
38. Komnitsas, K, Bartzas, G, Paspaliaris, I Efficiency of limestone and red mud barriers: laboratory column studies. *Miner Eng.* 2004;17:183-194.
39. Imran M, Asad M, Hadri SH, Mehmood S. Production and industrial applications of laccase enzyme. *J Cell Mol Biol.* 2012;10(1):1-11.
40. Eggert C. Laccase is responsible for antimicrobial activity of *Picnoporus cinnabarinus*. *Microbiol Res.* 1997;152:315-318.
41. Tychanowicz GK, de Souza DF, Souza CGM, Kadowaki MK, Peralta RM. Copper improves the production of laccase by the white-rot fungus *Pleurotus pulmonarius* in solid state fermentation. *Braz ArchBiol Techn.* 2006;49(5):699-704.
42. Greluk M, Hubicki Z. Kinetics, Isotherm And Thermodynamic Studies of reactive black 5 removal by acid acrylic resins. *Chem Eng J.* 2010;162(3):919-926.
43. Wo SW, Kim HJ, Choi SH, Chung BW, Kim KJ, Yun YS. Performance, kinetics and equilibrium in biosorption of anionic dye reactive black 5 by the waste biomass Of *Corynebacterium glutamicum* as a low-cost biosorbent. *Chem Eng J.* 2006;121:37-43.
44. Zhang GQ, Wanga YF, Zhang XQ, Ng TB, Wanga, HX. Purification and characterization of a novel laccase from the edible mushroom *Clitocybe maxima*. *Process Biochem.* 2010;45:627-33.
45. Tasgin E, Nadaroglu H. Purification and characterisation of laccase from *Lactarius volemus* and its application of removal phenolic compounds from some fruit juices, *Int J Food, Agr Env.* 2013;11(3&4 ):109-114.
46. Bradford MM. Rapid and sensitive method for the quantitation of microgram quantities of protein utilizing the principle of protein-dye binding. *Anal Biochem.* 1976;72:248-53.

47. Niku-Paavola, ML, Raaska, L, Itavaara, M Detection of white-rot fungi by a non-toxic stain. *Mycol Res.* 1990;94:27-31.
48. He, W, Zhan, H-Y, Wang, X-W, Wu, H An improved spectrophotometric procedure for the laccase assay. *J South China Univ Technol.* 2003;31:46-50.
49. Laemmli UK. Cleavage of structural proteins during the assembly of the head of bacteriophage. *Nature.* 1970;227:680-85.
50. Whitaker JR Determination of molecular weight of proteins by gel filtration on sephadex *Anal Chem.* 1963;35:1950-1953.
51. Castaldi P, Silveti M, Garau G, Deiana S. Influence of the pH on the accumulation of phosphate by red mud (a bauxite ore processing waste). *J Hazard Mater.* 2010;182:266-72.
52. Castaldi P, Silveti M, Santona L, Enzo S, Melis P. XRD, FT-IR, and Thermal analysis of bauxite ore-processing waste (red mud) exchanged with heavy metals. *Clay Clay Miner.* 2008;56:461-469.
53. Gok A, Omastova M, Prokes J. Synthesis and characterization of red mud/polyaniline composites: electrical properties and thermal stability. *Eur Polym J.* 2007;43:2471-2480.
54. Moon J, Deng Y, Flury M, Harsh JB. Cesium incorporation and diffusion in cancrinite, sodalite, zeolite and allophone. *Micropor Mesopor Mater.* 2005;86:277.
55. Nadaroglu H, Kalkan E, Dikbas N. Bacteria-Modified Red Mud for adsorption of cadmium ions from aqueous solutions. *Polish J Env Stud.* 2013;22(2):417-429.
56. Arami M, Limaee NY, Mahmoodi NM, Tabrizi NS. Removal of dyes from colored textile wastewater by orange peel adsorbent: Equilibrium and Kinetic studies *J Colloid Interf Sci.* 2005;288:371-376.
57. Kyzas, GZ A Decolorization technique with spent "Greek Coffee" grounds as zero-cost adsorbents for industrial textile wastewaters *Mater*, 2012;5:2069-2087
58. Slimani R, Anouzla A, Abrouki Y, Ramli Y, El Antri S, Mamouni R, Lazar S, El Haddad M. Removal of a cationic dye-methylene blue- from aqueous media by the use of animal bone meal as a new low cost adsorbent. *J Mater Env Sci.* 2011;2(1):77-87.
59. Malekbala MR, Hosseini S, Yazdi SK, Soltani SM, Malekbala MR. The Study of the potential capability o sugar beet pulp on the removal efficiency of two cationic dyes *Chem Eng Res Des*, 2012;90:704-712.
60. Larous S, Meniai AH, Lehocine MB Experimental study of the removal of copper from aqueous solutions by adsorption using sawdust *Desalination*, 2005;185:483-490.
61. Dotto GL, Pinto LAA. Adsorption of food dyes acid blue 9 and food yellow 3 onto chitosan: stirring rate effect in kinetics and mechanism. *J Hazard Mater.* 2011;187:164-170.
62. Mall ID, Srivastava VC, Agarwal NK. Removal of orange-g and methyl violet dyes by adsorption onto bagasse fly ash-kinetic study and equilibrium isotherm analyses. *Dyes Pigments.* 2006;69:210-223.
63. Pereira de Sa F, Cunha BN, Nunes LM. Effect of pH on the adsorption of sunset yellow FCF food dye into a layered double hydroxide (CaAl-LDH-NO3). *Chem Eng J.* 2013;215-216:122-127.
64. Kannan N, Veemaraj K. Removal of lead (II) Ions by adsorption onto bamboo dust and commercial activated carbons –A comparative study. *E-J Chem.* 2009;6 (2):247-256.
65. Hilal NM, Ahmed IA, Badr EE. Removal of acid dye (AR37) by adsorption onto potatoes and egg husk: a comparative study *J American Sci.* 2012;8(2):341-348.
66. Ahmaruzzaman M, Sharma DK. Adsorption of phenols from wastewater. *J Colloid Interf Sci.* 2005;287:14-24
67. Kanawade SM, Gaikwad RW. Removal of dyes from dye effluent by using sugarcane bagasse ash as an adsorbent. *Int J Chem Eng Appl.* 2011;2(3):202-206.



68. Setshedi K, Ren J, Aoyi O, Onyango MS. Removal of Pb (II) from aqueous solution using Hydrotalcite-like nanostructured material. *Int J Phys Sci.* 2012;7:63-72.
69. Wang L, Zhang J, Wang A. Fast removal of methylene blue from aqueous solution by adsorption onto chitosan-g-poly (acrylic acid)/attapulgitite composite. *Desalination.* 2011;266:33-39.
70. Sarkar K, Banerjee SL, Kundu PP. Removal of anionic dye in acid solution by self crosslinked insoluble dendronized chitosan. *Hydrol Curr Res.* 2012;3:133 DOI:104172/2157-75871000133.
71. Namasivayam C, Radhika R, Subha S. Uptake of dyes by a promising locally available agricultural solid waste: Coir Pith. *Waste Manag.* 2001;38:381-387.
72. Santhi T, Manonmani S, Smitha T. Removal of methyl red from aqueous solution by activated carbon prepared from the annona squamosa seed by adsorption. *Chem Eng Res Bull.* 2010;14:11-18.
73. Ofomaja AE, Ho YS. Equilibrium sorption of anionic dye from aqueous solution by palm kernel fibre as sorbent. *Dyes Pigments.* 2007;74:60-66.
74. Renault F, Morin-Crini, N, Gimbert, F, Badot, PM, Crini, G. Cationized starch-based material as a new ion-exchanger adsorbent for the removal of Cl acid blue 25 from aqueous solutions. *Biores Technol.* 2008;99:7573-7586.
75. Kumar PS, Ramakrishnan K, Gayathri R. Removal of Nickel (II) from aqueous solutions by ceralite IR 120 cationic exchange resins. *J Eng Sci Tech.* 2010;5:232-243.
76. Ho YS, McKay G. Pseudo-second order model for sorption processes. *Process Biochem.* 1999;34:451-465.
77. Janveja B, Sharma J, Kant K. Thermodynamic study of adsorption of amaranth dye on to steam activated pigmented rice husk carbon. *J Inter Acad Phys Sci.* 2011;15 (3):395-404.
78. Chakravarty S, Pimple S, Chaturvedi HT, Singh S, Gupta KK. Removal of copper from aqueous solution using newspaper pulp as an adsorbent. *J Hazard Mater.* 2008;159:396-403.
79. Suyamboo BK, Perumal RS. Equilibrium, thermodynamic and kinetic studies on adsorption of a basic dye by citrullus lanatus rind. *Iranica J Energ Env.* 2012;3(1):23-34.
80. Ramavandi B, Farjadfard S. Removal of chemical oxygen demand from textile wastewater using a natural coagulant. *Korean J Chem Eng.* 2014;31(1):81-87.
81. Asgari G, Ramavandi B, Farjadfard S. Abatement of azo dye from wastewater using bimetal-chitosan. *The Scientific World J;* 2013.
82. Asgari G, Ramavandi B, Sahebi S. Removal of a cationic dye from wastewater during purification by phoenix dactylifera. *Desalination and Water Treatment.* 2013;1-12.

© 2014 Nadaroglu et al.; This is an Open Access article distributed under the terms of the Creative Commons Attribution License (<http://creativecommons.org/licenses/by/3.0>), which permits unrestricted use, distribution, and reproduction in any medium, provided the original work is properly cited.

*Peer-review history:*

*The peer review history for this paper can be accessed here:*

<http://www.sciencedomain.org/review-history.php?iid=514&id=32&aid=4470>